Journal of

Pharmacology and Toxicology

aj

Academic
Journals Inc.

Molecular Modelling Analysis of the Metablism of Pyrazinamide

Fazlul Huq and Zahed Hossain
School of Biomedical Sciences, Faculty of Health Sciences,
The University of Sydney, Australia

Abstract: Tuberculosis is a global health problem of escalating proportions especially due to the prevalence of the acquired immunodeficiency syndrome (AIDS) that has greatly increased the incidence of the disease over the first few years. A commonly used front-line anti-tuberculosis drug is pyrazinamide (PZA) that causes dose-dependent hepatotoxicity, manifested by hepatocellular dysfunction. The exact of mechanism of action of PZA and that of its toxicity remain unclear. *In vivo*, PZA is metabolized in the liver to form the main metabolite pyrazinoic acid (PA) by enzymatic deamination. PA is oxidised by the action of xanthine oxidase (XO) to form 5-OH-PA which is the main excretory metabolite of PZA. PZA is also directly oxidised to form 5-OH-PZA by XO. A small amount of PU is produced by conjugation of PA with glycine. Molecular modelling analyses show that PZA and its metabolites may be subject to electrophilic attack at a number of sites including the two pyrazine ring nitrogens. Neither PZA nor any of its metabolites have very small HOMO-LUMO energy differences so that none is expected to be highly labile kinetically and none can be excluded from being the cause for the toxicity of PZA.

Key words: Pyrazinamide, tuberculosis, HIV, oxypurines, molecular modelling

Introduction

Tuberculosis (TB) caused by *Mycobacterium (M.) tuberculosis* is a global health problem of escalating proportions (Schon *et al.*, 1999). In 1990, over three million died of TB world-wide and eight million new cases of the disease were reported with 95% of them being in developing countries (Kochi, 1991) where the prevalence of the acquired immunodeficiency syndrome (AIDS) has greatly increased the incidence of the disease over the first few years (Nishimura *et al.*, 2004). There is a clear evidence that the incidence of multidrug-resistant TB is increasing (Chan and Neaton *et al.*, 1995). TB is considered to be a marker of social inequity and is a serious impediment to the economic development (Agarwal *et al.*, 2004). The drugs used in the treatment of TB are generally divided into two categories. The "first-line" agents, that combine good efficacy with acceptable levels of toxic side effects, include rifampicin, isoniazid and pyrazinamide (PZA) that are most widely used and often in combination (Gennaro *et al.*, 2001; Espinosa-Mansilla *et al.*, 2002). In the presence of microbial resistance or HIV infection, "second-line" drugs such as ethionamide and p-aminosalicylic acid must be used.

The recommended daily dose of PZA is 20-35 mg/kg/day in two equally divided doses. For adults this amounts to 750-1000 mg two times daily. Because of its lipid solubility, PZA is widely distributed throughout the body including the central nervous system. High concentrations of the drug are achieved in the liver, lung and kidneys. The drug is well absorbed after oral dose, reaching its peak serum concentration in 2 h. The serum half-life of PZA ranges from 10-16 h. PZA is eliminated in urine 4-14% as unchanged drug and the rest as metabolites formed in liver (Espinosa-Mansilla *et al.*, 2002). It can penetrate leukocyte membranes and is capable of killing intracellular organisms (Espinosa-Mansilla *et al.*, 2002; Winter, 2002).

Corresponding Author: Dr. Fazlul Huq, School of Biomedical Sciences, Faculty of Health Sciences,
The University of Sydney Australia P.O. Box 170, Lidcombe, NSW 1825, Australia
Tel: +061293519522   Fax: 061 293519520

Although PZA is characterized by high *in vivo* activity it shows poor *in vitro* activity, which is believed to be due to the difference between the *in vivo* tissue environment and the *in vitro* culture conditions (Somoskovi and Wade, 2004). It has been found that iron enhances the activity of PZA and its metabolite pyrazinoic acid (PA) against *M. tuberculosis*. However, the mechanism of iron enhancement of PA and PZA activity remains unknown. It is possible that iron causes lipid peroxidation of the *M. tuberculosis* membrane and membrane damage, leading to a disruption of membrane potential (Somoskovi and Wade, 2004).

It has been suggested that various factors such as pH, inoculum size, serum albnmin age, age of cultures and efflux inhibitors could influence the activity of PZA. PZA appears to kill semi-dormant bacilli persist in acidic environments inside macrophages (Heifes and Lindholm-Levy, 1992).

A common side effect of PZA is blocking the secretion of uric acid and other oxypurines in renal tubules. In order to avoid hyperuricaemia, xanthine oxidase (XO) inhibitors, such as allopurinol (which is a widely used in the treatment of gout), are given along with PZA (Kraemer *et al.*, 1998). PZA causes dose-dependent hepatotoxicity that is manifested by hepatocellular dysfunction. The toxicity generally disappears when the drug is withdrawn. Non-gouty arthralgia also commonly occurs that most often affects shoulders, knees and fingers. PZA is contraindicated in patients with a knee hypersensitivity to the drug.

In vivo, PZA is metabolized in the liver to form the main metabolite PA by enzymatic deamination (Salfinger *et al.*, 1990). PA is oxidised by the action of XO to form 5-hydroxypyrazinoic acid (5-OH-PA) which is the main excretory metabolite of PZA. PZA is also directly oxidised by XO to 5-hydroxypyrazinamide (5-OH-PZA) which on deamination produces 5-hydroxypyrazinoic acid (5-OH-PA) (Weiner and Tinker, 1972; Yamamoto *et al.*, 1987). A small amount of pyrazinuric acid (PU) is produced by conjugation of PA with glycine. The metabolites are eliminated in the urine by glomerular filtration. All available data suggest that the metabolite PA is the active compound against *M. tuberculosis* (Mehmedagic *et al.*, 2002) so that PZA may be considered as the prodrug. Acidic pH which facilitates the formation of PA is known to be essential for the activity of PZA (Herbert *et al.*, 1992).

Anti-tuberculosis drugs are prescribed for long periods of time and often in combination to retard the development of resistant strains (Nishimura *et al.*, 2004). However, drug combinations can cause pharmacokinetic interactions that may be associated with the induction or inhibition of drug-metabolizing enzyme cytochrome P450 (CYP). Whereas induction of CYP would result in increased elimination of a co-administered drug whose metabolism is mediated by the same isoenzymes, its inhibition would increase plasma concentration and toxicity of the concomitant drugs, especially the ones that have a narrow therapeutic window. For example, it is known that the antitubercolosis drug rifampicin (RF) is a well known inducer of several CYP isoenzymes (especially hepatic and intestinal CYP3A (Herbert *et al.*, 1992). RF has been reported to show unexpected interactions with clinically important drugs such as cyclosporine and nifedin and oral contraceptives such as phenytoin and theophylline (Herbert and Roberts, 1992; Venkatesan, 1992). However, PZA has not been found to cause any adverse drug interaction with co-administered drugs by the inhibition of CYP, even though its chemical structure is similar to that of isoniazid which is known to inhibit CYP1A2, CYP2A6, CYP2C19, CYP2C9 and CYP2E1 (Nishimura *et al.*, 2004).

Although PZA is a front-line anti-tuberculosis drug, its mechanism of action remains largely unknown. Nor do we have a complete knowledge on the toxicity of the drug. It has recently been reported that PZA inhibited the enkaryotic-like *fas I* gene (encoding fatty acid synthase I, FASI) in *M. tuberculosis* in correlation with its PZA susceptibility (Zimhony *et al.*, 2000]) The mycobacterial FASI generate C_{16} from acetyl-CoA primers, that is required for the biosynthesis of myocolic acid (Bloch, 1975). The acid is a key component of the mycobacterial cell wall, playing the important role of an effective lipophilic barrier to the penetration of some antibiotics. Antibiotics are generally more

active against multiplying bacteria and less effective against non-replicating bacteria as in the stationary phase or in the biofilm. As noted earlier, PZA is the opposite in the sense that it kills non-growing persisters more effectively than growing bacilli (Zhang *et al.*, 2003).

In this study, molecular modelling analyses have been carried out using the programs HyperChem 7.0 (HyperChem, 2002) and Spartan '02 (Spartan, 2002) to investigate the relative stability of PZA and its metabolites with the aim of obtaining an insight into the toxicity due to PZA and its metabolites (Fig. 1).

Computational Methods

The geometries of PZA and its metabolites PA, 5-OH-PZA, 5-OH-PA and PU have been optimised based on molecular mechanics, semi-empirical and DFT calculations, using the molecular modelling programs Spartan '02 and HyperChem 7.0. Molecular mechanics calculations were carried out using MM+ force field. Semi-empirical calculations were carried out using the routine PM3. DFT calculations were carried using the program Spartan '02 at B3LYP/6-31G* level. In optimization calculations, a RMS gradient of 0.001 was set as the terminating condition. For the optimised structures, single point calculations were carried to give heat of formation, enthalpy, entropy, free energy, dipole moment, solvation energy, energies for HOMO and LUMO. The order of calculations: molecular mechanics followed by semi-empirical followed by DFT minimized the chances of the structures being trapped in local minima rather than reaching global minima. To further check whether the global minimum was reached, some calculations were carried out with improvable structures. It was found that when the stated order was followed, structures corresponding to global minimum or close to that were reached in most cases. Although RMS gradient of 0.001 may not be sufficiently small for vibrational analysis, it is believed to be so for calculations associated with electronic energy levels. For the optimised structures, single point calculations were carried to give heat of formation, enthalpy, entropy, free energy, dipole moment and solvation energy, HOMO and LUMO.

Results and Discussion

Table 1 gives the total energy, heat of formation as per PM3 calculations, enthalpy, entropy, free energy, dipole moment, energies of HOMO and LUMO as per both PM3 and DFT calculations for PZA and its metabolites PA, 5-OH-PZA, 5-OH-PA and PU. Fig. 2-6 give the optimised structures of PZA and its metabolites PA, 5-OH-PZA, 5-OH-PA and PU as per PM3 calculations using the program HyperChem 7.0. The structures also give (a) 2D contours of total electrostatic potential and (b) 2D HOMO plots. The dotted arrows in (a) indicate positions of most negative electric potential and in (b) the locations of HOMOs with the greatest electron densities.

Table 1: Calculated thermodynamic and other parameters of pyrazinamide and its metabolites

Molecule	Calculation type	Total energy (kcal mol^{-1}/ atomic unit*)	Heat of formation (kcal mol^{-1})	Enthalpy (kcal mol^{-1} K^{-1})	Entropy (cal mol^{-1} K^{-1})
Pyrazinamide	PM3	-9.67	3.92	68.59	86.18
	DFT	-433.04		69.89	85.32
Pyrazinoic acid	PM3	-60.35	-48.20	61.24	85.53
	DFT	-452.90		62.10	82.74
5-Hydroxypyrazina-mide	PM3	-59.78	-44.35	72.87	91.41
	DFT	-508.28		73.36	90.24
5-Hydroxypyrazi-noic acid	PM3	-111.01	-96.72	65.55	90.79
	DFT	-528.14		65.54	87.69
Pyrazinuric acid	PM3	-139.12	-120.84	115.74	105.23
	DFT	-736.13		103.55	109.76

Table 1: Continued

Molecule	Solvation energy (kcal mol^{-1} K^{-1})	Free energy (kcal mol^{-1})	Dipole moment (debye)	HOMO (eV)	LUMO (eV)	LUMO-HOMO (eV)
Pyrazinamide	-13.60	42.89	3.31	-10.17	-1.01	9.16
	-10.97	44.45	3.79	-6.79	-1.93	4.86
Pyrazinoic acid	-12.14	35.74	4.53	-10.70	-1.36	9.34
	-9.35	37.43	4.78	-7.38	-2.42	4.96
5-Hydroxypyrazina-mide	-15.42	45.62	2.59	-10.08	-0.94	9.14
	-13.50	46.45	2.70	-6.79	-1.71	5.08
5-Hydroxypyrazi-noic acid	-14.30	38.48	4.33	-10.38	-1.26	9.12
	-12.08	39.40	4.80	-7.41	-2.16	5.25
Pyrazinuric acid	-23.55	84.37	5.54	-10.25	-1.24	9.01
	-48.40	70.82	6.87	-6.89	-2.23	4.66

* in atomic units from DFT calculations
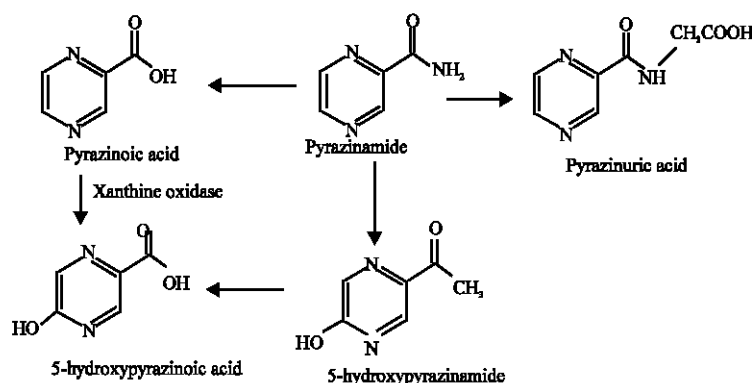
Fig. 1: Proposed metabolic pathways for pyrazinamide and its metabolites (Based on Heifes and Lindholm-Levy, 1992)

The calculated solvation energies of PZA and its metabolites PA, 5-OH-PZA, 5-OH-PA and PU from DFT calculations in kcal mol^{-1} are, respectively -10.97, -9.35, -13.50, -14.30 and -48.40 and their dipole moments from DFT calculations are 3.79, 4.78, 2.70 4.80 and 6.87, respectively. The values indicate that PZA and or any of its metabolites would have some solubility in water. It was noted earlier that PZA also dissolves in lipids. This means that PZA would be neither quite lipophilic nor quite hydrophilic. As expected, PU, the conjugated product of PA with glycine has the largest solvation energy value and hence the compound is expected to have the highest solubility in water.

The calculated heat of formation of PA is -48.20 k cal mol^{-1} as compared to that for PZA of 3.92 k cal mol^{-1}. The very large difference in heat of formation values (a large negative value for PA and a small positive value for PZA) suggest the change in Gibb's free energy (ΔG) for the conversion: PZA$^-$PA would be negative so that the process could be thermodynamically spontaneous. From similar considerations it may be concluded that the conversion of 5-OH-PZA into 5-OH-PA would also be spontaneous.

PZA and its four metabolites have LUMO-HOMO energy differences ranging from 4.67 to 5.25 eV from DFT calculations suggesting that the compounds would differ in their kinetic lability. PU is expected to be most labile whereas 5-OH-PA would be least labile kinetically. PU would however be expected to have the smallest biological half-life since it would be most readily excreted in the urine.

In the case of PZA, PounA, 5-OH-PZ and 5-PH-PA, the electrostatic potential is found to be more negative ard the two pyrazine ring nitrogen atoms and the carbonyl oxygen atom, indicating that the positions may be subject to electrophilic attack. In the case of 5-OH-PA, the electrostatic potential
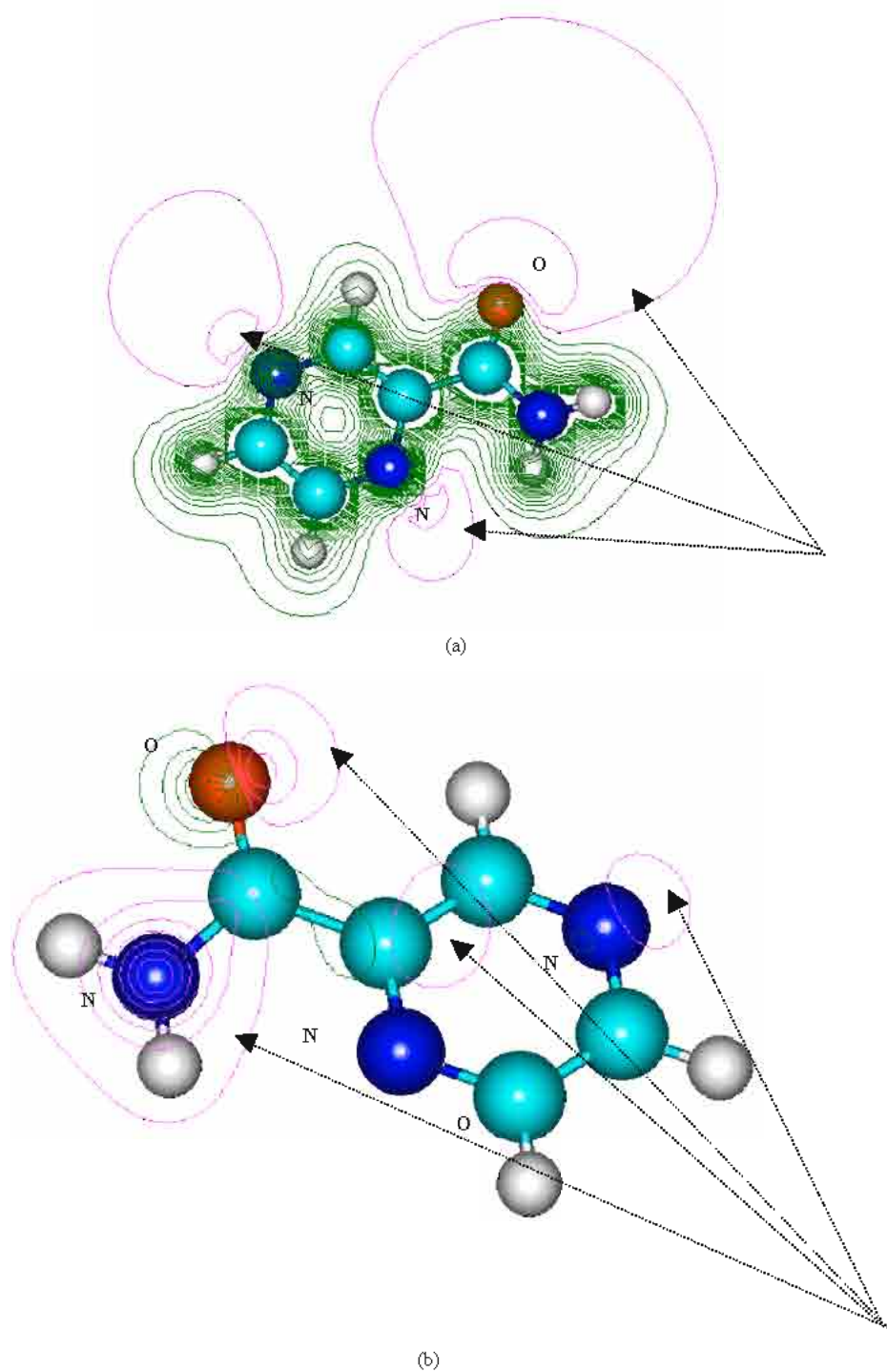
(a)

(b)

Fig. 2: Structure of pyrazinamide giving (a) 2D contours of total electric potential and (b) 2D HOMO plot
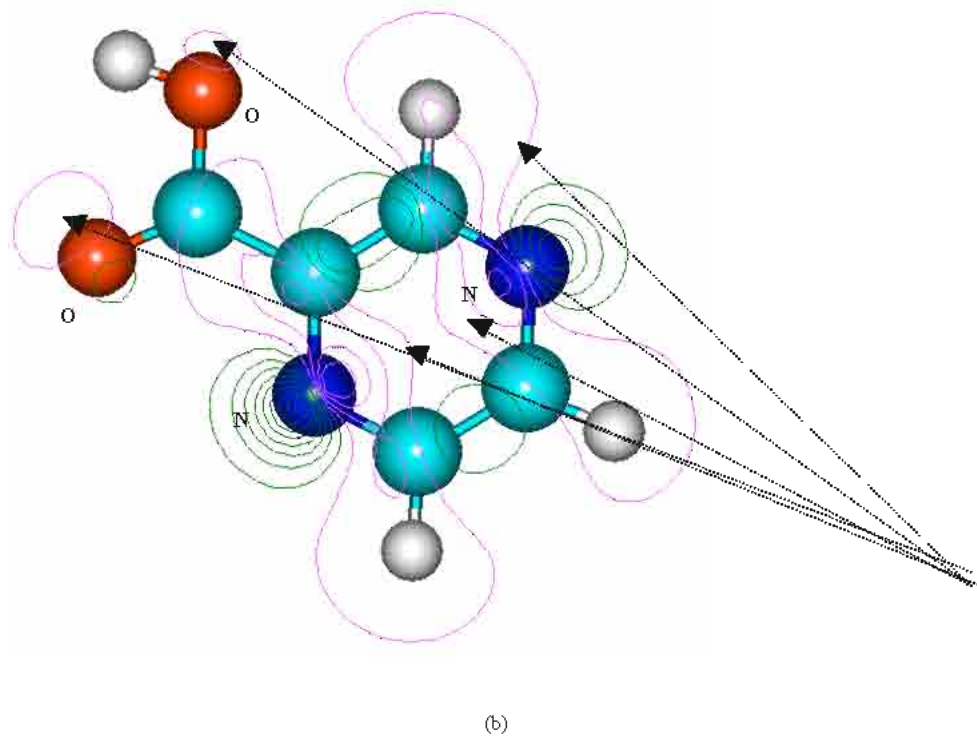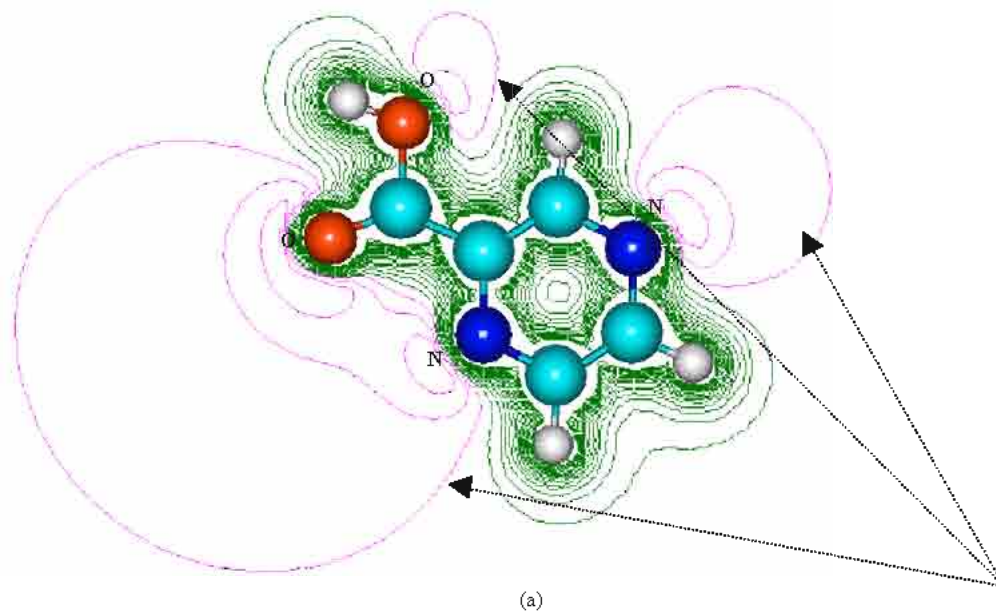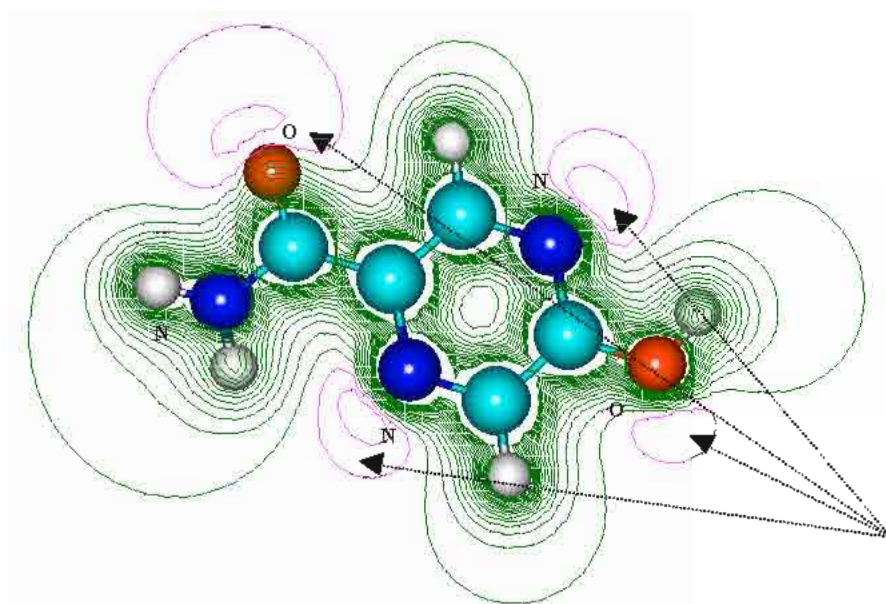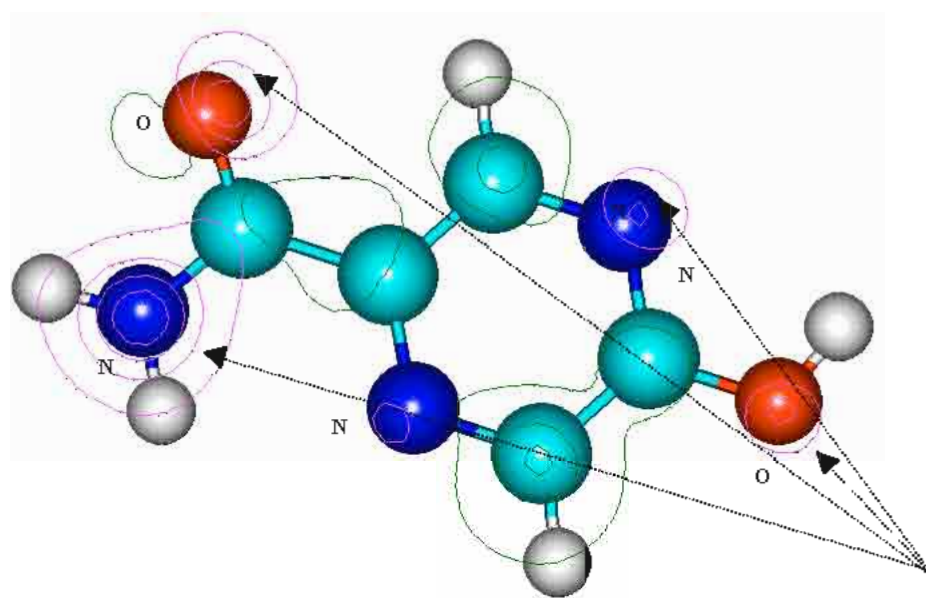
(a)

(b)

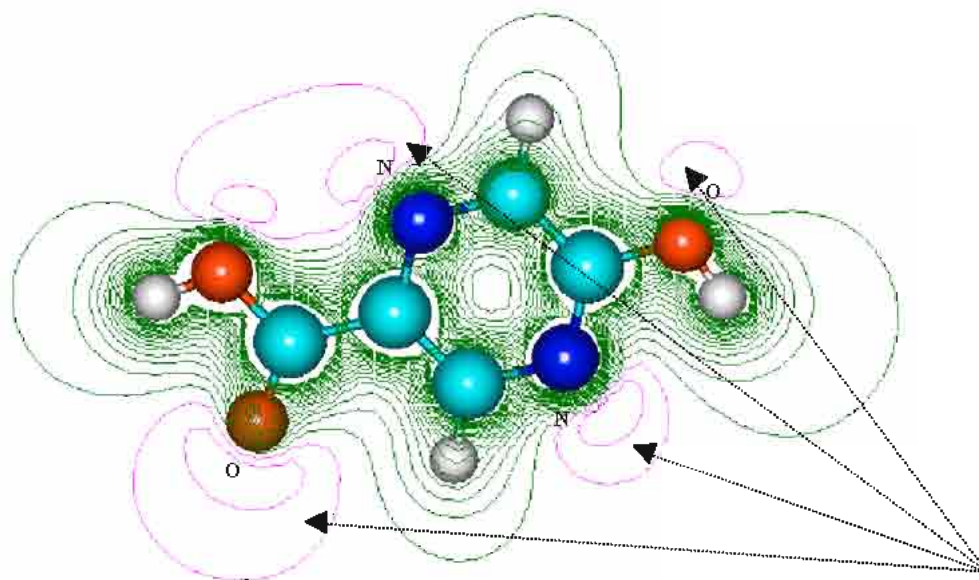Fig. 3: Structure of pyrazinoic acid giving (a) 2D contours of total electric potential and (b) 2D HOMO plot
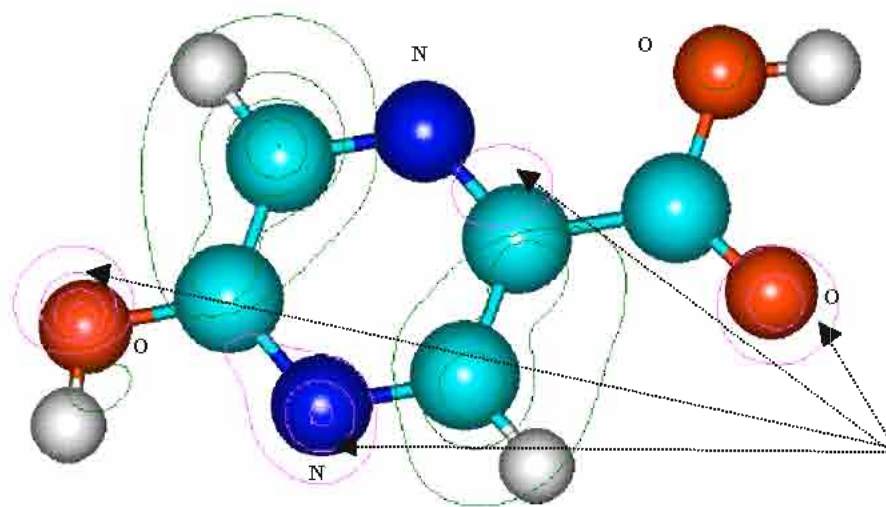
(a)

(b)

Fig. 4: Structure of 5-hydroxypytazinamide giving (a) 2D contours of total electric potential and (b) 2D HOMO plot
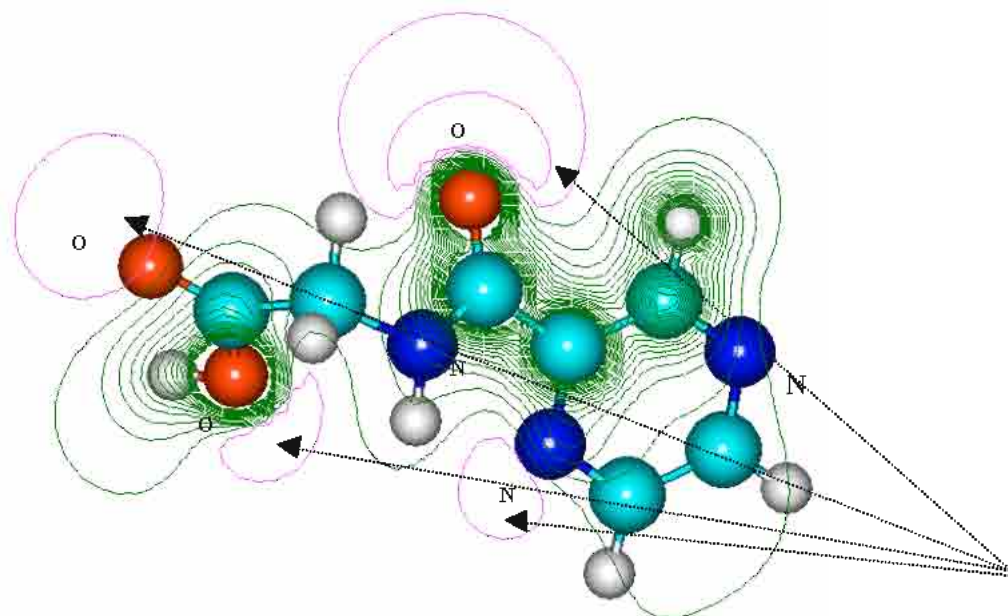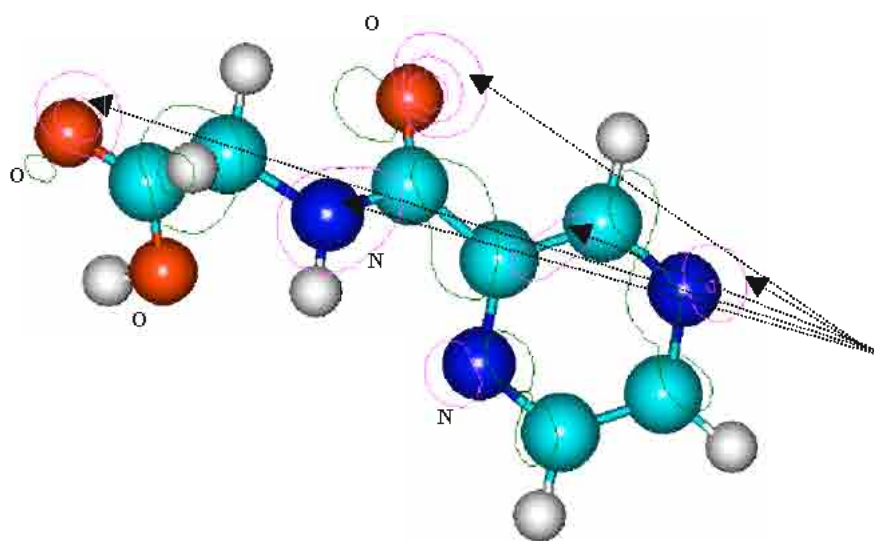
(a)

(b)

Fig. 5: Structure of 5-hydroxypyrazinoic acid giving (a) 2D contours of total electric potential and (b) 2D HOMO plot

(a)

(b)

Fig. 6: Structure of pyrazinuric acid giving (a) 2D contours of total electric potential and (b) 2D HOMO plot

is found to be negative also around the oxygen atoms of the carboxyl group and the hydroxyl group attached to the pyrazine ring carbon atom at the fifth position. In the case of PU, the electrostatic potential is found to be more negative around one pyrazine ring nitrogen atom and the carbonyl oxygen atom of the amide linkage and the carboxyl oxygen atoms, indicating that the positions may be subject to electrophilic attack

In the case of PZA, the HUMOs with large electron density are found to be centered on the carbonyl oxygen, the amide nitrogen, a carbon and a nitrogen atom of the pyrazine ring. In the case of PA, the HUMOs with large electron density are found to be centered on a number of atoms including two nitrogen atoms and a ring carbon atom of the pyrazine ring, the carbonyl and the hydroxyl oxygens of the carboxyl group. In the case of 5-OH-PZA, the HUMOs with large electron density are found to be centered on the amide nitrogen, carbonyl oxygen, hydroxyl oxygen and a pyrazine ring nitrogen atom. In the case of 5-OH-PA, the HUMOs with large electron density are found to be centered on the carbonyl oxygen, hydroxyl oxygen and a pyrazine ring nitrogen atom. In the case of PU, the HUMOs with large electron density are found to be centered on a number of atoms including a pyrazine ring nitrogen atom, the carbonyl oxygen, nitrogen atom of the glycine moiety and the carboxyl group oxygens of the glycine moiety.

Conclusions

Molecular modelling analyses show that PZA and its four metabolites have LUMO-HOMO energy differences ranging from 4.67 to 5.25 eV from DFT calculations suggesting that the compounds would differ in their kinetic lability. However, none of the metabolites is expected to be extremely labile. Thus, it is not possible to exclude PZA and any of its metabolites from being the cause of toxicity.

Acknowledgments

References

Agarwal, S., I. Singh, K.J. Kaur, S.R. Bhade, C.L. Kaul and R. Pachagnula, 2004. Comparative bioavailability of rifampicin, isoniazid and pyrazinamide from a four drug fixed dose combination with separate formulations at the same dose levels. Intl. J. Pharmaceut., 276: 41-49.

Bloch, K., 1975. Fatty acid synthases from *Mycobacterium phlei*. Methods Enzymol., 35: 84-90.

Chan, I.S., J.D. Neaton, L.D. Saravolatz, L.R. Crane and J. Osterberger, 1995. Frequencies of opportunistic diseases prior to death among HIV-infected persons. AIDS, 9: 1145-1151.

Espinosa-Mansilla, A., M.I. Acedo-Valenzuela, A.M. de la Pena, F.C. Canada and F.S. Lopez, 2002. Determination of antituberculosis drugs in urine and pharmaceuticals by LC using a gradient flow combined with programmed diode array photometric detection. Talanta, 58: 273-280.

Gennaro, M.C., R. Canvino and C. Abrigo, 2001. Ion interaction reagent reversed-phase high performance liquid chromatography determination of anti-tuberculosis drugs and metabolites in biological fluids. J. Chromatogr. B, 754: 477-486.

Heifes, L. and P. Lindholm-Levy, 1992. Pyrazinamide sterilizing activity *in vitro* against semi-dormant *Mycobacterium tuberculosis* bacterial populations. Ann. Rev. Respir. Dis., 145: 1223-1225.

Herbert, M.F., J.P. Roberts, T. Prueksaritanont and L.Z. Benet, 1992. Bioavailability of cyclosporine with concomitant rifampin administration is markedly less than predicted by hepatitic enzyme induction, Clin. Pharmacol. Ther., 52: 453-457.

HyperCube HyperChem, Release 7 for Windows, 7.0 ed., HyperCube, Ed., 2002.

Kochi, A., 1991. The global situation and the new control strategy of the World Health Organization. Tubercle, 72: 1-6.

Kraemer, H.J., U. Feltkamp and H. Breithaupt, 1998. Quantification of pyrazinamide and its metabolites in plasma by ionic-pair high performance liquid chromatography. Implications for separation mechanism. J. Chromatogr. B, 706: 319-328.

Mehmedagic, A., P. Verite, S. Menager, C. Tharasse, C. Chabenat, D. Andre and O. Lafont, 2002. Investigation of the effects of concomitant caffeine administration on the metabolic Disposition of Pyrazinamide in Rats, Biopharm. Drug Dispos., 23: 191-195.

Nishimura, Y., N. Kurata, E. Sakurai and H. Yasuhara, 2004. Inhibitory effect of antituberculosis drugs on human cytochrome P450-Mediated Activities. J. Pharmacol. Sci., 96: 41-49.

Salfinger, M., A.J. Crowle and L.B. Reller, 1990. Pyrazinamide and pyrazinoic acid activity against tubercle bacilli in cultured human macrophages and in the BACTEC system, J. Infect. Dis., 162: 201-207.

Schon, T., N. Gebre, T. Sundqvist, G. Aderaye and S. Britton, 1999. Effects of HIV co-infection and chemotherapy on the urinary levels of nitric oxide metabolites in patients with pulmonary tuberculosis. Scand. J. Infect. Dis., 31: 123-126.

Somoskovi, A., M.A. Wade, Z. Sun and Y. Zhang, 2004. Iron enhances the antituberculosis activity of pyrazinamide. J. Antimicrob. Chemther., 53: 192-196.

Spartan '02 Wavefunction, Inc. Irvine, CA, USA, 2002.

Venkatesan, K., 1992. Pharmacokinetic drug interactions with rifampicin. Clin. Pharmacokinet., 22: 47-65.

Weiner, I.M. and J.P. Tinker, 1972. Pharmacology of pyrazinamide: Metabolic and renal function studies related to the mechanism of drug induced urate retention. J. Pharmacol. Exp. Ther., 180: 411-434.

Winter, J.C., 2002. In: Textbook of Pharmacology. Smith, C.M. and A.M. Reynard (Eds.). W.B. Saunders, Philadelphia, USA., pp: 867-868.

Yamamoto, T., Y. Moriwaki, S. Takahashi, T. Hada and K. Higashino. 5-Hydroxypyrazinamide, a human metabolite of pyrazinamide. Biochem. Pharmacol., 36: 3317-3318.

Zhang, Y., M. Wade, A. Scorpia, H. Zhang and Z. Sun, 2003. Mode of action of pyrazinamide: Disruption of *Myobacterium tuberculosis* membrane transport and energetics by pyrazinoic acid. J. Antimicrob. Chem., 52: 790-795.

Zimhony, O., J.S. Cox, J.T. Welch, C. Vilcheze and W.R. Jacobs Jr., 2000. Pyrazinamide inhibits the eukaryotic-like fatty acid synthase I (FASI) of the Mycobacterium tuberculosis. Nat. Med., 6: 1043-1047.